

# Metastable state dynamics and power law relaxation in a supercooled liquid

Sudha Srivastava and Shankar P. Das

*School of Physical Sciences, Jawaharlal Nehru University, New Delhi 110067, India*

(Received 3 January 2000; revised manuscript received 5 July 2000; published 19 December 2000)

We consider glassy relaxation by using a model for supercooled liquid where the usual set of hydrodynamic variables is extended to include the presence of very slowly decaying defect densities. The long time limit of the density correlation function, the nonergodicity parameter, is studied in the vicinity of the dynamic transition point, and scaling exponents with respect to the distance from the critical point are obtained. In addition to the usual square root cusp, we also see a linear dependence on distance from transition with respect to the metastability parameters. We analyze the power law relaxation of the density correlation function at the initial stage of the dynamics, and obtain an exponent dependent on temperature. Results are compared with data obtained from light scattering experiments.

DOI: 10.1103/PhysRevE.63.011505

PACS number(s): 64.70.Pf, 64.60.Cn

## I. INTRODUCTION

The self-consistent mode-coupling [1–3] approximation for the memory function is particularly useful in understanding cooperative effects in a dense liquid. It predicts a two step relaxation process for glassy dynamics involving a power law decay of the dynamic density correlation over intermediate time scales crossing over to the stretched exponential behavior in the long time, termed the  $\alpha$  relaxation. In an extended version of mode coupling theory [4,5], there is a final exponential relaxation mode of the density correlation function, restoring the ergodicity over the longest time scales. The mechanism restoring the ergodicity was obtained as a result of coupling of density fluctuations with currents in a compressible liquid. This final decay mode presumably relates to the presence of defects or free volumes in the amorphous system. In the present paper we describe an extension of a simple mode coupling formalism with the inclusion of the extra slow mode of defect density that develops in the amorphous state. We consider the coupled dynamics of the defect mode and the density fluctuations with the proper wave vector dependence. Modeling of a supercooled liquid in terms of vacancies was first done in the free volume theory of Cohen and Grest. The idea of liquidlike and solidlike clusters was introduced from a phenomenological picture of a supercooled liquid, to model the transport phenomena in an amorphous system [6]. This mainly involved associating some free volume or void with individual units in the cluster structure of the liquids. The movement of the free volumes was considered crucial for transport in the liquid. A dynamic percolation theory was used to predict that at some critical density the transport process is completely frozen, giving rise to very long relaxation times. In a hydrodynamic approach, the transport properties of the isotropic fluid is considered through dynamical equations for the conserved modes which arise as a direct consequence of the microscopic conservation laws in the system [7]. The hydrodynamic description for crystals as well as liquid crystals involved extending the set of slow variables in the system to include Nambu-Goldstone modes due to symmetry breaking. The additional slow variable that was introduced was the displacement vector for the different lattice sites. The con-

sideration of the dynamics of the vacancies in a crystal from a unified hydrodynamic approach was proposed by Martin, Parodi, and Pershan [8], and was further developed by Cohen *et al.* to describe linear transport in a crystal [9] and also an amorphous solid [10].

In the present work we consider the defect mode in a spirit similar to that introduced in Refs. [11,12]. The mode coupling contributions to the transport coefficients are obtained from the extended set of hydrodynamic equations, including the dynamics of the defect mode. The liquidlike state persists up to densities much higher than the critical density, where simple mode coupling theory (MCT) will predict a sharp transition. In the extended model, instead of a single dynamic transition at a critical density, a line of transition is obtained as a function of the packing fraction and the strength of the coupling to the defect density. Following Ref. [11] we assume that the defects move in a metastable potential, and we assume a simple two level model for the defect potential. We consider the nonergodicity parameter, which is the long time limit of the density correlation function for the supercooled liquid beyond the ideal transition point, and we obtain scaling laws corresponding to a different choice of thermodynamic parameters, very close to the transition. Next we study the dynamics to consider the initial power law relaxation of the density correlation function over an intermediate time range in the presence of a very slowly decaying defect mode. Thus the role of the structure of the liquid as well as the coupling of the defect mode to the density fluctuations over the so called  $\beta$ -relaxation regime is probed. From the solution of the mode coupling equations for the density correlation function, we obtain the temperature dependence and the wave vector dependence of the power law exponents of the relaxation.

The paper is organized as follows. In Sec. II we briefly describe the model considered. In Sec. III we consider predictions from the mode coupling equations in the asymptotic limit, and the consequent phase diagram with respect to the coupling constants. Here we also show the scaling behavior of the nonergodicity parameter near the transition. In Sec. IV we obtain solutions to the dynamical equations for the structure factor in the initial power law regime, and obtain the temperature dependent exponents. We end the paper with a short discussion of the results.

## II. THE MODEL STUDIED

The Laplace transform of the density correlation function normalized with respect to its equal time value is represented in terms of the generalized transport coefficient  $\Gamma(q, z)$  as

$$\psi(q, z) = \frac{z + i\Gamma(q, z)}{z^2 - \Omega_q^2 + iz\Gamma(q, z)}, \quad (1)$$

where  $\Omega_q = q/\sqrt{\beta m S(q)}$  is the characteristic microscopic frequency of liquid dynamics, and  $S(q)$  is the static structure factor. In simple mode coupling theory  $\Gamma(q, z)$  is expressed self consistently in terms of slowly decaying density correlation functions, resulting in a feedback mechanism on the transport properties. The enhancement of the transport coefficient depends on the strength of the mode coupling contributions expressed in terms of the structure factor of the liquid. If the Percus-Yevick solution for a hard sphere system with a Verlet-Weiss correction is used for the structure factor, the dynamic transition occurs at  $\eta = 0.524$ . This simple mode coupling model for the supercooled liquid dynamics can be obtained from an analysis of the equations of fluctuating nonlinear hydrodynamics. Here one takes into account the nonlinear equations for the conserved modes, and renormalizations of the transport coefficients are computed. These models were further extended [13,14,11,12] to include the extra slow mode of the defect density, to describe the solid-like nature of the supercooled liquid. In the present work the approach in Ref. [12] is followed to obtain a coupled set of equations for the dynamics. The defect density  $n(\vec{x}, t)$  is taken to be similar to the mass density in its Poisson brackets [15] with other hydrodynamic variables. The resulting corrections to the transport coefficient are given in terms of the mode coupling integrals [12]

$$\Gamma^{mc}(q, t) = \frac{1}{\beta m} \int \frac{d\vec{k}}{(2\pi)^3} [V^{(1)}(q, k)\psi(k, t) + V^{(2)}(q, k)\psi(k, t)\psi(q-k, t)], \quad (2)$$

where the mode coupling vertices as obtained by Yeo with full wave vector dependence are given by

$$V^{(1)}(q, k) = \frac{1}{n_0} [2yqU(q, k)s(k)s(q-k) + q^2\kappa n_0 c(k)s(k)] + O(\mu) \quad (3)$$

and

$$V^{(2)}(q, k) = \frac{1}{2n_0} [U^2(q, k) - 2yqU(q, k)]s(k)s(q-k) + O(\mu). \quad (4)$$

Here the vertex function  $U(q, k)$  is given by

$$U(q, k) = n_0[\hat{q} \cdot kc(k) + \hat{q} \cdot (q-k)c(q-k)], \quad (5)$$

with  $n_0$  as the particle number density. These results are obtained with a free energy functional which has a typical kinetic part [16], followed by a ‘‘potential’’ part given by

$$\begin{aligned} \beta m F = & \int d\vec{x} \rho \{\ln(\rho/\rho_0) - 1\} \\ & - \frac{1}{2m} \int d\vec{x} d\vec{x}' \delta\rho(x)c(x-x')\delta\rho(x') \\ & + \int d\vec{x} h[n(x)] + F_{\text{int}}. \end{aligned} \quad (6)$$

The functional  $h[n(x)]$  corresponds to the defect potential, and  $F_{\text{int}}$  is the defect-mass density interaction term. Following Ref. [12] we take this to have a form with the parameters  $\mu$  and  $\nu$  characterizing the shape of the potential well in terms of second and third derivatives, respectively;  $\mu = \bar{n}^2 h''(\bar{n})$  and  $\nu = \bar{n}^3 h'''(\bar{n})$ . The extrema of the potential occur at  $n = \bar{n}$ , such that  $h'(\bar{n}) = 0$ . The potential well is characterized in terms of two dimensionless parameters  $y$  and  $\kappa$ ,

$$y \equiv \frac{\nu}{n_0 k_B T}, \quad \kappa \equiv \frac{\nu^2 x}{\mu^2}, \quad (7)$$

where  $n_0$  is particle number density. The defect and mass density interaction part of the effective Hamiltonian  $F_{\text{int}}$  is given as

$$F_{\text{int}} = B \int d\vec{x} d\vec{x}' \delta n(x)c(x-x')\delta\rho(x'). \quad (8)$$

Here we have treated the defect density as if it is similar to the mass density variable.  $B$  is a constant giving the strength of the coupling between the defects and the particle density. We define a dimensionless quantity  $x = B\rho_0 \bar{n}/n_0 k_B T$  as a measure of this coupling. In the model considered here, the defect density  $n$  is weakly interacting with the mass density ( $n_0$ ). The above result, [Eq. (2)] reduces to the standard result [17] for the one component system if the defect density mode is ignored. The presence of a linear term in the mode coupling vertex comes about through this coupling with a very slowly varying defect correlation [18]. A wave vector independent schematic model containing a linear density correlation function term—the so called  $\phi_{12}$  [19] model—was originally proposed to obtain stretched exponential behavior in the long time relaxation of supercooled liquids. In this formulation of the MCT, the ergodicity restoring mechanism that finally takes over for the final relaxation in the system is ignored. However, even in the idealized model, instead of a dynamic transition at a critical density, a line of transition is obtained as a result of the coupling to the defect density. In Sec. III, we will consider the behavior of the nonergodicity parameter in the vicinity of the dynamic transition. In the present formulation we compute the scaling behavior close to the transition in terms of the different parameters for the defect well potential. Finally, we consider a dynamical equation for the density correlation

function, and compute the exponent of the power law relaxation. We obtain the dependence of this exponent  $a$  on the density as well as the wave vector.

### III. IMPLICATIONS OF THE IDEAL TRANSITION

The ideal glassy state is characterized by the property that the density correlation function freezes to a nonzero value in the asymptotic limit. We consider model equations in the long time limit over which the defect correlation is taken as a constant. In order to identify the ideal transition from an ergodic phase to a nonergodic phase, we consider the non-zero solution for the density correlation function in this limit for all  $q$  values. We use the definition  $\psi(q, t \rightarrow \infty) = f(q)$  as the nonergodicity parameter. In the long time or  $z \rightarrow 0$  limit, Eq. (1) reduces to

$$\frac{f(q)}{1-f(q)} = \int \frac{d^3k}{(2\pi)^3} \times [V^{(1)}(q, k)f(k) + V^{(2)}(q, k)f(k)f(q-k)], \quad (9)$$

where vertices  $V^{(1)}$  and  $V^{(2)}$  are given by Eqs. (3) and (4). These set of coupled equations are solved self-consistently for  $f(q)$  over a  $q$  grid starting from zero, to a maximum cutoff using numerical integration. A set of critical parameters  $(\kappa_c, y_c, \eta_c)$  is identified below in which all  $f(q)$ 's converge to zero values (ergodic phase), and above that critical point all  $f(q)$ 's converge to nonzero values (nonergodic phase). The solution of  $f(q)$ 's in the nonergodic phase can then be used to study the scaling properties of the nonergodicity parameter. We use the Perkus-Yevick solution, with the Verlet-Wiess correction for the hard sphere structure factor in the mode coupling integrals. The wave vector grid  $N = 300$  and the upper cutoff for integration  $\Lambda\sigma = 50$  was chosen. The critical value of the packing fraction that marks the transition from an ergodic phase to a nonergodic phase is calculated, keeping  $\kappa$  and  $y$  fixed. The critical points  $(y_c, \kappa_c, \eta_c)$  in  $\kappa$ - $\eta$  phase space are located by fixing  $y_c$  and varying  $\eta$  and  $\kappa$ , and those in  $y$ - $\eta$  phase space by fixing  $\kappa_c$  and varying  $y$  and  $\eta$ . The phase diagrams for both cases are shown in Figs. 1(a) and 1(b), respectively. The behavior of the long time limit of the density correlation function or the so called nonergodicity parameter was very widely investigated close to the ideal transition point. The set of integral equations (9) was solved for a number of densities in the nonergodic phase, i.e., densities higher than the corresponding critical density  $\eta_c = 0.525$  for  $\kappa_c = 0.0021$  and  $y_c = 0.05$ . Variation of  $f(q) - f_c(q)$  as a function of distance from the transition point, i.e.,  $\epsilon_\eta = (\eta - \eta_c)/\eta_c$ , is shown in Fig. 2(a) for a wave vector equal to the peak of the static structure factor. The dashed line shows the fit to a square root cusp law,

$$f(q) = f_c(q) + Ah_1(q)\epsilon_\eta^{1/2}, \quad (10)$$

while the solid line shows the fit with an exponent dependent on the wave number  $q$ . In the range of  $\epsilon$  beyond 0.01, the fit with the  $q$  dependent exponent is better than that for the

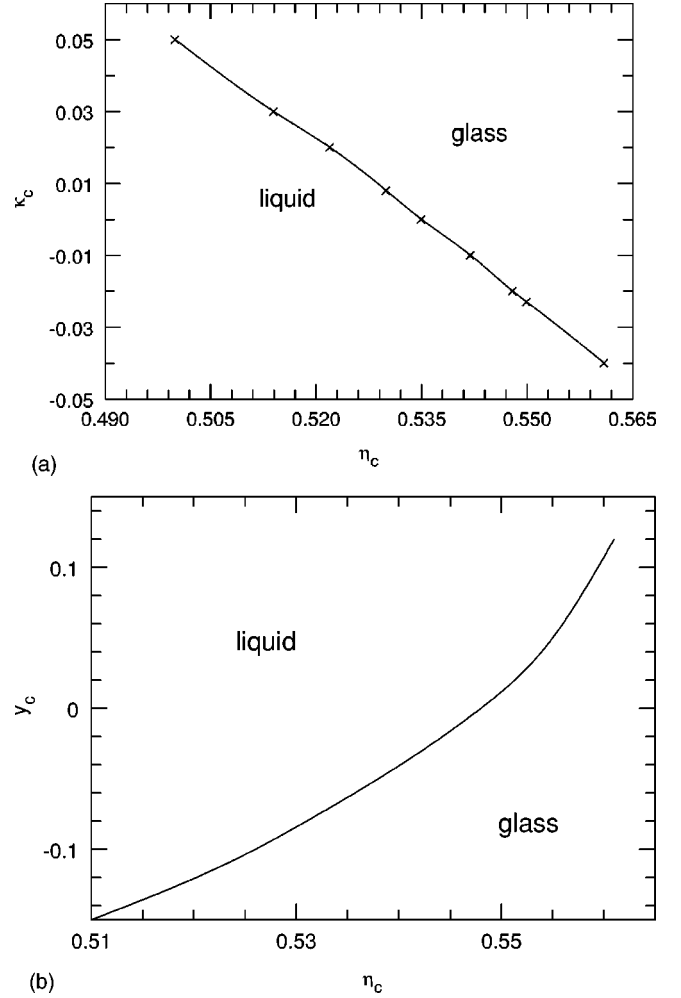


FIG. 1. Phase diagram in (a)  $\eta$ - $\kappa$  space at  $y_c = 0.12$ , and (b)  $\eta$ - $y$  space at  $\kappa_c = 0.0027$ .

square root cusp, even after adding an  $O(\epsilon)$  correction to the latter. Figures 2(b) and 2(c) show a variation of  $f(q) - f_c(q)$  with respect to the coupling parameters  $\kappa$  and  $y$ . Here  $\epsilon_\kappa = (\kappa - \kappa_c)/\kappa_c$ , and so on. Both  $\kappa$  and  $y$ , which are parameters related to the metastable potential well for the defect motion, scale as *linear* dependences on the distance from the transition. This is in contrast to the square root cusp in the *same* relative distance from the transition  $\epsilon$  with respect to the density. This holds within the range for the corresponding  $\epsilon \leq 0.005$ , beyond which the addition of an  $O(\epsilon^2)$  correction gives a good fit [solid lines in Figs. 2(b) and 2(c)]. The contribution from the  $O(\epsilon^2)$  correction is  $\approx 10$ – $15$ %. This linear behavior of  $f(q)$  with respect to the metastability parameters  $\kappa$  and  $y$  for the defect density, in the same  $\epsilon$  range as that of  $\epsilon_\eta$ , is a new result from the present model, to our knowledge. The stability matrix for  $\kappa$ ,  $y$ , and  $\eta$  in the extended model for the memory function with the linear term needs to be analyzed in order to ascertain the relative strength of the different order terms with respect to these variables. The numerical results show here that the linear term dominates in the  $\epsilon$  range considered here with respect to the variables  $\kappa$  and  $y$ .

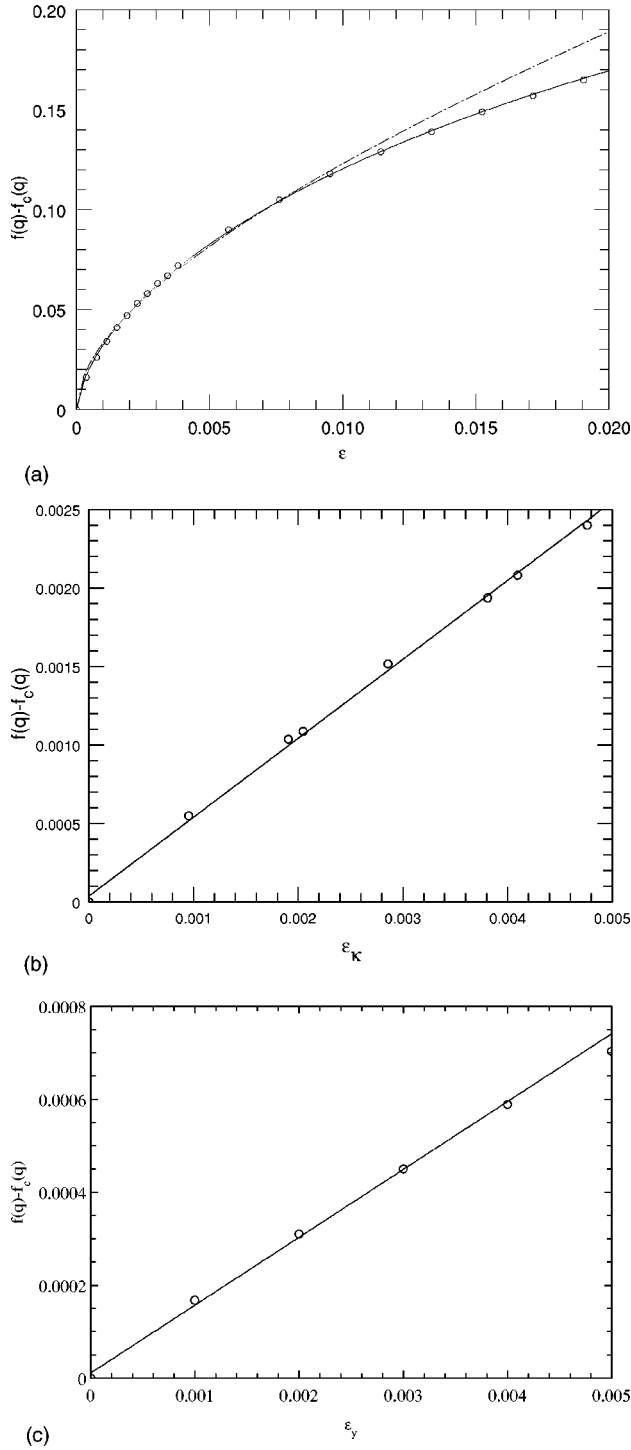


FIG. 2. (a)  $f(q)$  (circles) as a function of distance from the transition point  $\epsilon_\eta$  at the peak of the structure factor for critical parameters  $\eta_c=0.525$ ,  $y_c=0.05$ , and  $\kappa_c=0.0021$ . The dashed line shows the fit to a square root cusp law [Eq. (10)] (see the text); the solid line shows the fit with an exponent dependent on the wave vector. (b)  $f(q)$  (circles) as a function of distance from the transition point  $\epsilon_\kappa$  for the same wave vector and critical parameters, as stated in (a). The solid line shows the linear dependence. (c)  $f(q)$  (circles) as a function of distance from the transition point  $\epsilon_y$  for the same wave vector and critical parameters as stated in (a). The solid line shows the linear dependence.

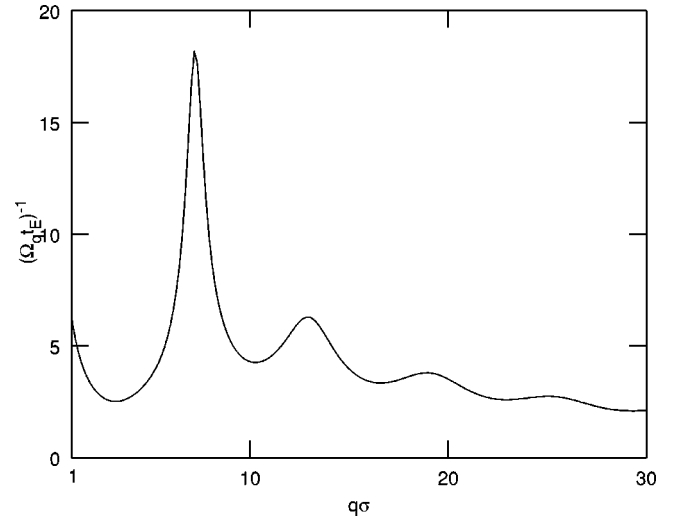


FIG. 3. Variation of the time scale  $(\Omega_q t_E)^{-1}$  as a function of wave number  $q\sigma$  for a packing fraction  $\eta=0.561$ .

#### IV. POWER LAW RELAXATION

In Sec. III we studied the long time limit of the density correlation function. In this section the dynamical behavior of fluids at the initial stage for time scales larger than that for the microscopic frequencies are considered. To study the dynamic properties we solve the mode coupling equation obtained from Eq. (1) for the supercooled liquid dynamics:

$$\begin{aligned} \dot{\psi}(q,t) + \Gamma_0(q)\psi(q,t) + \Omega_q^2\psi(q,t) \\ + \int_0^t d\tau \Gamma(q,t-\tau)\psi(q,\tau) = 0. \end{aligned} \quad (11)$$

The density correlation function  $\psi(q,t)$  is computed as a solution of the extended mode coupling equation.  $\psi(q,t)$  was evaluated over a mesh of  $q$  values for a particular density. For microscopic time scales  $t < \Omega_q^{-1}$ , the dynamics is governed by a bare transport coefficient. The present study is in the so called  $\beta$  relaxation regime. Results from mode coupling models as well as experimental studies showed that the density correlation function shows a power law relaxation. In the MCT model that we study here, this behavior is valid for time scales longer than the corresponding microscopic time scale given by  $(\Omega_q t_E)^{-1}$ . In Fig. 3 this time scale  $(\Omega_q t_E)^{-1}$  is plotted as a function of wave vector  $q$  for a packing fraction  $\eta=0.561$ . All the calculations in this section correspond to times *above*  $(\Omega_q t_E)^{-1}$ .

In the extended model that we consider, the density correlation function does not freeze beyond the critical transition point  $\eta=0.525$  of the ideal MCT, and fluid remains in the ergodic phase. The equation for both ideal ( $\kappa=0.0, y=0.0$ ) and extended mode coupling models ( $\kappa=-0.04, y=0.12$ ) has been solved at packing fraction  $\eta=0.561$ . In the ideal case, the system freezes such that all  $f(q)$ 's converge to a nonzero value (nonergodic phase) at this density. In Fig. 4 we show the evaluation of  $\psi(q,t)$  with time  $(t/\tau_0)$  by a dotted line for the simple model, while for the extended model the solid line shows the behavior of  $\psi(q,t)$ . The unit



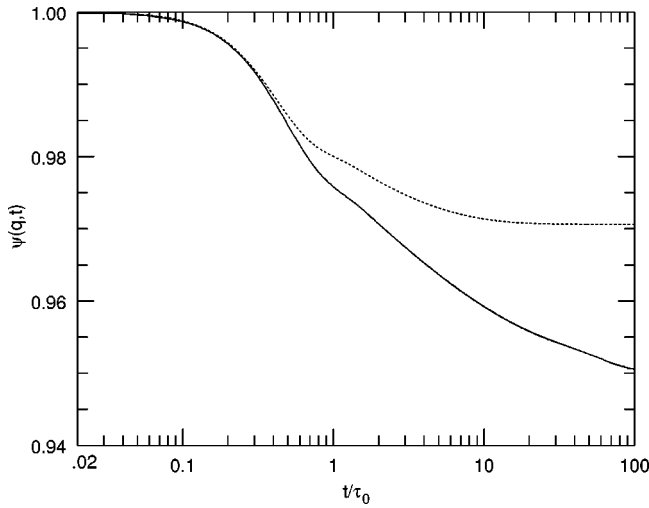


FIG. 4. Decay of the density correlation function  $\psi(q,t)$  as a function of time  $t/\tau_0$  at the wave vector peak of the structure factor for  $\eta=0.561$ . In the ideal model (dotted lines), this freezes to a constant value (glassy state), while in the present model (solid line) it decays to a liquidlike state.

of time is chosen as  $\tau_o = 10t_E$ . As seen in Fig. 4, the present model predicts a liquidlike (ergodic phase) at densities as high as  $\eta=0.561$ . The liquidlike behavior is facilitated by the motion of the defect densities in the metastable potential well. The change in the shape of the defect's metastable potential well as a function of particle density is investigated along the critical surface of Figs. 1(a) and 1(b). In Fig. 5 we show the change in the shape of the potential well with these values of  $y$  and  $\kappa$ . As the packing fraction  $\eta$  increases,  $y$  also increases, making the potential well deeper. The barrier height for the defects increases with increasing  $\eta$ , and results in a trapping of the defects in the potential well over long time scales in the nonergodic state. In a way this demonstrates that, although the final ergodicity restoring processes removes this sharp transition, some remnant of this transition

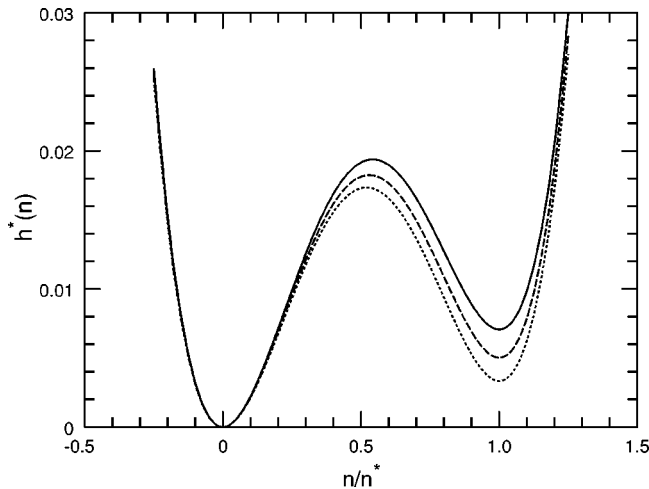


FIG. 5. Variation of the depth of the potential with  $n/n^*$  for  $\eta_c$  0.525 (solid line), 0.538 (dashed line), and 0.549 (dotted line). In the figure,  $h^*(n)$  represents the dimensionless quantity  $h(n)\beta\epsilon n\sigma^3$ .

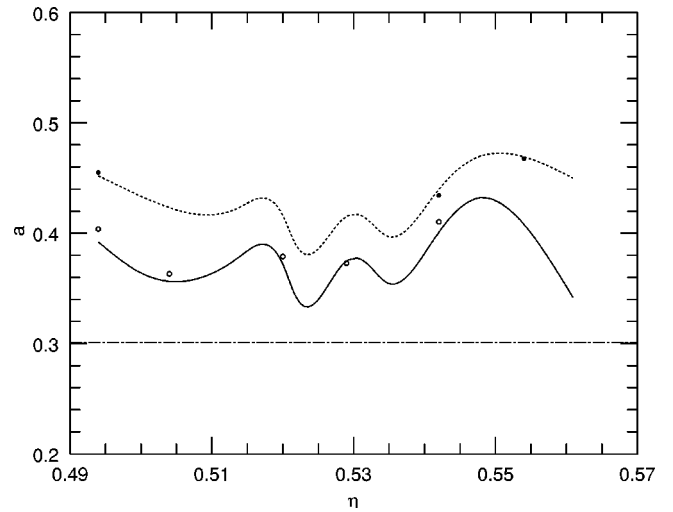


FIG. 6. Variation of the exponent  $a$  as a function of density at the peak of the structure factors  $q_m$  (solid line) and  $0.63q_m$  (dashed line). The horizontal dash-dotted line corresponds to the temperature independent exponent  $a=0.301$ , as predicted from simple MCT. Open and filled circles are power law exponents as obtained from fitting the data from Ref. [20] at  $q_m$  and  $0.63q_m$  respectively. Metastability parameters used for obtaining the theoretical curves (solid and dashed lines) are indicated by points in Fig. 1(a).

is seen, with a slow relaxation of the density correlation function due to the feedback effects.

As discussed earlier, in this model there is not just a single transition point but a series of transition points in the  $\kappa$ - $y$  phase space. To study the relaxation dynamics as a function of density, we solve Eq. (11) for  $\psi(q,t)$  for  $\eta$  values very close to the points along the transition line shown in Fig. 1(a). The critical parameters  $y$  and  $\kappa$ , related to the potential for the defect density and its coupling to the density fluctuations along this line, are used for evaluating the mode coupling integrals. The potential well shapes for the defect density where  $\psi(q,t)$  is evaluated, in a few cases, are shown in Fig. 5. From the solution of the mode coupling equation, we directly obtain the exponent  $a$  as a function of packing fraction  $\eta$  fitting to the form,

$$\psi(q,t) = f_c(q) + Ch(q)(t/t_o)^{-a} \quad (12)$$

where  $C$  is a constant, and  $t_o$  is the time scale over which the power law relaxation persists. The density dependence of the power law exponents calculated from the solution of extended MCT equations are shown in Fig. 6 for two different wave vectors, namely, the peak of the static structure factor ( $q_m$ ) (solid line) and at  $0.63q_m$  (dashed line). Metastability parameters  $\kappa$  and  $y$ , used for obtaining the theoretical curves (solid and dashed lines), are indicated by state points in Fig. 1(a). To investigate the agreement of these predictions for the power law exponents shown in Fig. 6, we fit the light scattering data reported in Figs. 5(a) and 5(b) of Ref. [20] to Eq. (12), and obtain the exponent. In Fig. 6, we indicate that the exponents computed from our analysis of the experimental data for different densities at the corresponding wave vectors, show good agreement. In the same figure we also show

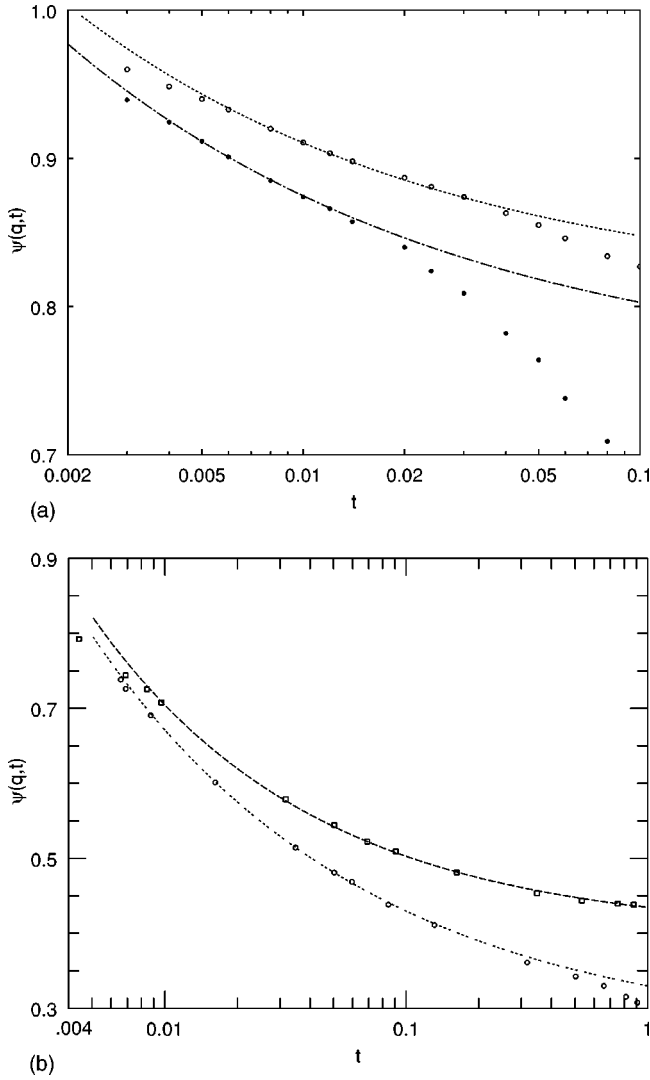


FIG. 7. (a) Normalized intermediate scattering function  $\psi(q,t)$  vs delay time  $t$  in seconds for the data obtained from Ref. [20] at a peak of the static structure factor ( $q_m$ ) for  $\eta=0.529$  (filled circles) and 0.542 (open circles). Dashed lines show the power law fit. NEP values are obtained with  $\kappa=0.008$  for  $\eta=0.529$ ,  $\kappa=-0.01$  for  $\eta=0.542$ , and  $y=0.12$  for both densities. (b) Normalized intermediate scattering function  $\psi(q,t)$  vs delay time  $t$  in seconds for the data obtained from Ref. [20] at  $0.63q_m$  for  $\eta=0.554$  (filled circles) and 0.542 (open circles). Dashed lines show the power law fit.  $\kappa=-0.03$  and  $y=0.12$  are used for the NEP calculation at  $\eta=0.554$ .

the density independent exponent as predicted from simple MCT. The quality of the fit is presented in Figs. 7(a) and 7(b). The fit at  $q_m$  for two different densities  $\eta=0.529$  (filled circles) and 0.542 (open circles) is shown in Fig. 7(a) by dashed lines. The same fit for  $0.63q_m$  is shown in Fig. 7(b) for  $\eta=0.554$  (filled circles) and 0.542 (open circles). We also consider the wave vector dependence of the exponent  $a$ . In Fig. 8, we show the exponent  $a$  as computed from the solution of the model equations at  $\eta=0.561$  for different wave vectors. The minimum occur at peak of the structure factor showing the characteristic slow relaxation at this wave vector. Before ending this section, we like to emphasize two points here.

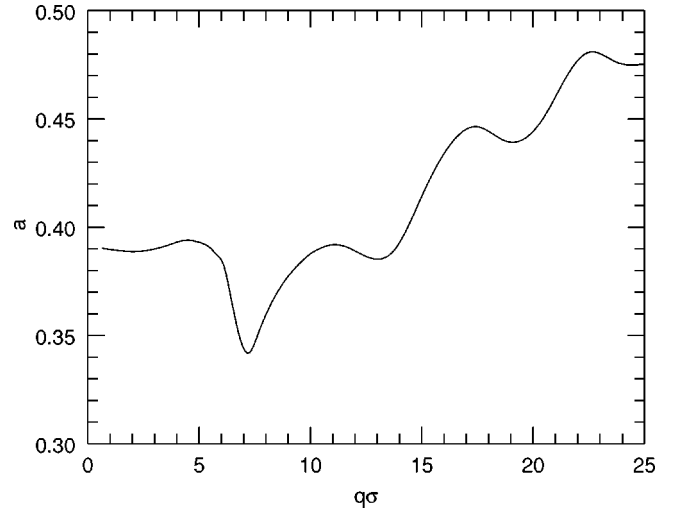


FIG. 8. Variation of the exponent  $a$  as a function of the wave vector  $q\sigma$  for a packing fraction  $\eta=0.561$  and corresponding  $\kappa_c = -0.04$  and  $y_c=0.12$ .

(i) The theoretical exponents reported in Fig. 6 are indeed predictions from the model equations *at the densities* indicated in the figure, in terms of the relevant transition point. Unlike Ref. [21], *we do not need to map to another equivalent density* to account for the discrepancy in the transition point that exists between experimental and simple MCT results.

(ii)  $f_q^c$  for a fixed density depend on the metastability parameters  $\kappa$  and  $y$  on the transition surface. Thus variation of  $f_q^c$  with critical parameters follows naturally from the model equations, and there is no need to adjust the  $f_q^c$  in any ad hoc way to compare with experimental data.

## V. DISCUSSION

In the present work we consider the model proposed by Yeo [12] using a fluctuating hydrodynamic description for the fluid to include the defect density  $n(x)$  reflecting the freezing of the local structures in the amorphous solid. The dynamics of the defect density is constructed, assuming it to be variable similar to the mass density as far as the microscopic dynamics is concerned. Following Ref. [12], we work with an effective Hamiltonian for the system that is compatible with the properties of the amorphous solid. Although the defect density  $n(x)$  field signifies freezing on a local length scale, isotropy is assumed for the system for long length scales.

The asymptotic behavior for the mode coupling equations are considered to obtain the phase diagrams. Through coupling to the defect density, the relaxation time can increase, although the liquid does not freeze into an ideal glassy phase even for a much higher packing fraction than the critical value of the transition as predicted from a simple mode coupling model with only density fluctuations. In the generic vicinity of the critical surface the NEP (nonergodicity parameter) exhibits a square root singularity in the ideal MCT. However, in the extended model with different vertex functions we focus on a range in the vicinity of the transition

point that is typically used in experiments to study the behavior of the NEP. What we show here is that in this range, which is quite relevant to the experiments, we do see a linear behavior with respect to the metastability parameters  $\gamma$  and  $\kappa$ , while at the *same* relative distance from the transition with respect to the density a variable cusp behavior is valid.

Next we turn to a discussion of the behavior of the power law exponent. In conventional MCT, the transition occurs at a lower density ( $\eta_c = 0.525$ ) than predicted from the experiments ( $\eta_c = 0.565$  [20]). However, this was largely ignored, and comparison between theoretical results with the experiment have been done in terms of the “distance” from the transition  $\epsilon$ . In the ideal MCT there is a single power law exponent independent of temperature. The numerical solution to the MCT equations indicate that the single scaling form fails as we move away from the transition. For this one needs to add more and more correction terms [22] to the scaling form as the distance from the ideal transition increases. On the other hand, here we have taken a different approach to the problem. Through the formulation of the extended model we show that the system can avoid freezing at higher densities than predicted from the ideal MCT. A power law exponent, which follows, is naturally dependent on density. We have taken the data of Ref. [20] and fitted the power law exponent, and this agrees well with the theoretical predictions. We would like to stress here that unlike the ideal MCT, with a temperature independent exponent, we *do not* need to adjust the transition point to obtain agreement with experimental data. Finally we discuss the wave vector dependence of the power law exponent. Analyzing the solutions of the MCT equations from our model here for different  $q$  values, we find the exponents of power law relaxation to be dependent on the wave vector. This shows a good agreement with data at two different wave vectors. Here we would like to mention that even solutions of ideal MCT equations will better fit a  $q$  dependent exponent, as was demonstrated by

one of the present authors in Ref. [23]. However, this will imply that the nonperturbative solution of the MCT equations will violate the so-called factorization property, which demands that the density correlation function completely separates out its wave vector and time dependence—a result that is even stronger than dynamic scaling. Indeed, if one resorts to adding more and more correction terms, it is still possible to maintain a  $q$  independent exponent, but we believe this would mean imposing a strong condition while the actual model equations indicate a different behavior. The present extension, in terms of the defect density, thus allows more parameters in the theory. While this is a phenomenological approach, it accounts for the temperature dependence of the power law exponent from a microscopic model. In the present work we have shown that the predictions from proposed model equations—without assuming factorization property—do show good agreement with experimental results.

The amorphous solidlike nature of the supercooled liquid is essential for conceiving the presence of defect density in addition to the usual hydrodynamic modes. Since the transition points are shifted, one obtains a power law relaxation with a density (temperature) dependence in the exponent. The model considered in the present work can be extended to the  $\alpha$ -relaxation regime, where the combined role of the density fluctuation and the defect fluctuation will be considered. The diffusive mode which restores ergodicity in the supercooled liquid, final decay can be linked with the motion of vacancies or free volumes in the amorphous solids. Thus the defect density mode and mass density essentially behave in a similar way in their asymptotic relaxation regimes.

#### ACKNOWLEDGMENTS

S.S. acknowledges the support of SRF from UGC. S.P.D. acknowledges the support of the NSF under Project No. INT9615212.

- 
- [1] B. Kim and G. F. Mazenko, Phys. Rev. A **45**, 2393 (1992).
  - [2] Transp. Theory Stat. Phys. **24** (6-8) (1995) special issue on subject, edited by S. Yip and Paul Melman.
  - [3] W. Götze in *Liquids, Freezing and the Glass Transition*, edited by D. Levisque, J. P. Hansen, and J. Zinn-Justin (Elsevier, New York, 1991).
  - [4] S. P. Das and G. F. Mazenko, Phys. Rev. A **34**, 2265 (1986).
  - [5] R. Schimitz, J. W. Dufty, and P. De, Phys. Rev. Lett. **71**, 2066 (1993).
  - [6] M. H. Cohen and G. S. Grest, Phys. Rev. B **20**, 1077 (1979).
  - [7] D. Forster, *Hydrodynamic Fluctuations, Broken Symmetry and Correlation Functions* (Benjamin, Reading, MA, 1975).
  - [8] P. C. Martin, O. Parodi, and P. S. Pershan, Phys. Rev. A **6**, 2401 (1972).
  - [9] P. D. Fleming, III and C. Cohen, Phys. Rev. B **13**, 500 (1976).
  - [10] C. Cohen, P. D. Fleming, and J. H. Gibbs, Phys. Rev. B **13**, 866 (1976).
  - [11] J. Yeo and G. F. Mazenko, J. Non-Cryst. Solids **172-174**, 1 (1994); Phys. Rev. E **51**, 5752 (1995).
  - [12] J. Yeo, Phys. Rev. E **52**, 853 (1995).
  - [13] S. P. Das and R. Schilling, Phys. Rev. E **50**, 1265 (1994).
  - [14] S. P. Das and S. Srivastava, Phys. Lett. A **266**, 58 (2000).
  - [15] I. E. Dzyloshinski and G. E. Volvick, Ann. Phys. (N.Y.) **67**, 125 (1980).
  - [16] J. Langer and L. Turski, Phys. Rev. A **8**, 3230 (1973).
  - [17] U. Bengtzelius, W. Gotze, and A. Sjölander, Phys. Rev. E **50**, 1265 (1994).
  - [18] B. Kim, Phys. Rev. A **46**, 1992 (1992).
  - [19] W. Gotze and L. Sjögren, Rep. Prog. Phys. **55**, 241 (1992).
  - [20] W. van Meegen and P. N. Pusey, Phys. Rev. A **43**, 5429 (1991).
  - [21] W. Götze and L. Sjögren, Phys. Rev. A **43**, 5442 (1991).
  - [22] T. Franosch, M. Fuchs, W. Götze, M. R. Mayr, and A. P. Singh, Phys. Rev. E **55**, 7153 (1997).
  - [23] S. P. Das, J. Chem. Phys. **98**, 3328 (1993).